

Molten Globule Unfolding Monitored by Hydrogen Exchange in Urea<sup>†</sup>

Aaron K. Chamberlain and Susan Marqusee\*

Department of Molecular and Cell Biology, 229 Stanley Hall, University of California, Berkeley, Berkeley, California 94720-3206

Received October 30, 1997; Revised Manuscript Received December 23, 1997

**ABSTRACT:** The molten globule state of *Escherichia coli* ribonuclease H1 was studied by hydrogen exchange in order to understand how the energetics of individual regions react to the presence of denaturant. Hydrogen exchange rates were monitored (1) directly by NMR spectroscopy and (2) indirectly by quenching the exchange process and returning to the native state for NMR detection. Direct hydrogen exchange on the molten globule state demonstrated that the observed protons exchange 3–100-fold more slowly than in an unfolded peptide. The quenched hydrogen exchange experiments were modeled after the recently developed “native state hydrogen exchange” experiment and were carried out as a function of urea concentration. The free energy of hydrogen exchange varied linearly with denaturant concentration for all 29 measurable protons, suggesting that each amide’s exchange behavior can be modeled with only one type of opening transition. The free energy of unfolding measured by hydrogen exchange and corresponding *m* values varied for each residue implying a noncooperative molten globule structure. These results are in contrast to similar exchange experiments on native proteins which generally display more than one type of exchange behavior. The single type of exchange seen in the molten globule is probably due to its larger conformational freedom and noncooperative nature.

Attempts to understand how proteins fold into their native structure naturally lead to questions about the intermediate, partially folded conformations along a kinetic or thermodynamic pathway of protein folding. Partially folded conformations populated at equilibrium, so-called molten globules, have been shown to have the same general characteristics as early kinetic intermediates populated transiently during the folding process (1, 2). In some cases, the two have been shown to have the same regions of structure (3, 4). Understanding the energetics of the molten globule unfolding will help to identify the stabilizing interactions that dictate this partially folded state and illuminate important features governing the process of protein folding.

Molten globule states of proteins are ensembles of flexible, highly mobile structures which are compact, but lack a well-packed, specific core (1). Recent hydrogen exchange experiments on molten globule states have demonstrated that only a particular region of each protein shows protection from exchange (slower hydrogen exchange rates than in an unstructured peptide) (5–7). Hence, only a select region is presumed to be structured. Select regions of structure have also been detected during the kinetics of protein folding (8, 9) and in the presence of chaperonins (10–13). The protection factors observed in these folded regions are often small (hundreds) reflecting the low stability of these partially folded

states. These exchange measurements, however, only begin to address the unfolding energetics of individual residues. In particular, we do not understand how specific regions of partially folded proteins react to the presence of denaturant.

Measurements of amide hydrogen exchange rates as a function of some environmental change, such as denaturant, can also be used as a tool for determining the energetics of individual regions within a protein (14–21). Under some conditions (EX2<sup>1</sup> kinetics) hydrogen exchange rates can be used to determine the free energy of an opening reaction. These exchange studies, however, can be complicated. Exchange of protected protons can occur by at least two different opening mechanisms: unfolding events and local fluctuations. If a proton exchanges through unfolding events, the exchange rate is sensitive to denaturant and the opening reaction allowing exchange is promoted by denaturant. This denaturant sensitivity implies a change in exposed surface area during the opening event (22). If the exchange rate is independent of denaturant concentration, the proton exchanges through what we define as a local fluctuation. Thus, the addition of denaturant, or other environmental change, is necessary for determining whether exchange is dominated by small local fluctuations or by larger unfolding events.

<sup>†</sup> This work was supported by grants from the NIH (GM 50945) and the Arnold and Mabel Beckman Foundation.

\* To whom correspondence should be addressed. E-mail: marqusee@zebra.berkeley.edu.

<sup>1</sup> Abbreviations: RNase H, *E. coli* ribonuclease H1 with three free cysteines replaced by alanine; NMR, nuclear magnetic resonance; CD, circular dichroism; HSQC heteronuclear single quantum coherence; 1D, one-dimensional; 2D, two-dimensional; EX1, first-order exchange kinetics; EX2, second-order exchange kinetics; HX, hydrogen exchange.

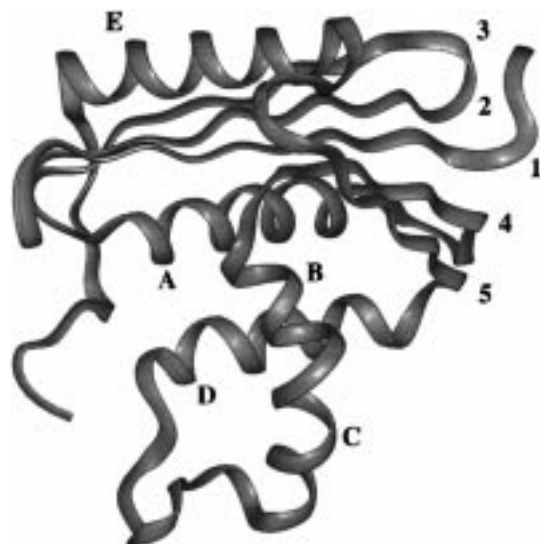


FIGURE 1: Ribbon diagram of wild-type *E. coli* RNase H (37). Letters A–E mark the five helices and the numerals 1–5 are located on the right edge of the  $\beta$  strands.

To investigate the energetics which determine the molten globule ensemble of structures, we used the low pH state (pH 1) of *Escherichia coli* ribonuclease H1 (RNase H). Previous work on the acid state of RNase H (6) has shown it to have all the characteristics of a molten globule: (1) partial secondary structure formation, (2) some degree of compactness, (3) a loosely packed hydrophobic core which binds hydrophobic dyes, and (4) a lack of fixed tertiary interactions (7). The structured regions of this ensemble were elucidated using a quenched hydrogen exchange method in the absence of denaturants (6). The most protected, or structured, region of the protein is helix A, with considerable protection also seen in helices D, B, and E and strand 4 (Figure 1). Since the acid state of RNase H is soluble to  $\sim 1$  mM in low salt conditions, direct NMR studies of the molten globule are also feasible.

Here, we have investigated how the individual regions of the molten globule of RNase H unfold in the presence of denaturants and the energetics that describe these opening reactions. To validate the quenched hydrogen exchange method, we carried out initial hydrogen exchange studies directly on the molten globule using one-dimensional proton NMR spectroscopy. To study the unfolding energetics of the RNase H molten globule, we carried out quenched exchange studies with increasing amounts of urea which detect exchange using 2D heteronuclear NMR spectroscopy on the native state.

## MATERIALS AND METHODS

**Materials.** Deuterium oxide,  $^{15}\text{N}$  ammonium chloride, deuterated buffers, acids, and bases were purchased from Isotec. All other buffer reagents were purchased from Sigma or Fischer. Deuterated urea was prepared by dissolving protonated urea in  $\text{D}_2\text{O}$ , rotary evaporating the  $\text{D}_2\text{O}$ , and redissolving 4 times.

**Protein Preparation.** For this study we used a variant of *E. coli* ribonuclease H1, RNase H\* (herein referred to as simply RNase H), with all three free cysteines replaced by alanine. This variant has activity and stability indistinguishable from the true wild-type protein. RNase H was expressed

and purified as described by Dabora et al. (6) except that the purified protein was dialyzed into 200 mM  $\text{NH}_4\text{HCO}_3$  (not 50 mM) before lyophilization and storage at 4 °C.

**Circular Dichroism (CD) Spectroscopy.** Urea denaturation of the molten globule state of RNase H was monitored at 4 °C in a deuterated solution at pD 0.8 (in this and all other experiments, pD of deuterated solutions has been corrected for the effect of glass electrodes (23)). Samples were prepared by adding increasing amounts of a solution containing 40  $\mu\text{g}/\text{mL}$  RNase H, 10 mM phosphoric acid, 50 mM KCl, 8.3 M urea, 3.5 M DCl, pD 0.8 in  $\text{D}_2\text{O}$  to a similar solution containing 0 M urea and 0.13 M DCl, pD 0.8. The large excess of DCl in the 8 M urea solution was necessary due to the buffering capacity of urea at this pD. All components were deuterated except the RNase H. Each sample was equilibrated for at least 2.3 min in an Aviv 62DS spectrometer, and the CD signal at 222 nm was averaged for 30 s.

**Direct NMR and Hydrogen Exchange Measurements on the Molten Globule.** All NMR spectra were taken on a Bruker DMX 600 MHz spectrometer. Data acquisition for the heteronuclear single quantum coherence (HSQC) spectrum (24–26) of the molten globule state of RNase H (10 mg/mL RNase H in 10 mM phosphoric acid, 50 mM potassium chloride, 120 mM hydrochloric acid with 10%  $\text{D}_2\text{O}$ , pH 1) was carried out at 5 °C. The HSQC spectra were processed as described previously (27).

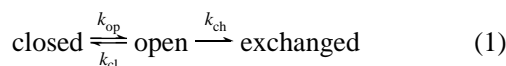
For direct hydrogen exchange measurements, 9 mg of  $^{15}\text{N}$ -labeled RNase H was dissolved in 550  $\mu\text{L}$  of 10 mM phosphoric acid and 150 mM DCl in  $\text{D}_2\text{O}$ , pD 0.9, at 4 °C and spun for 1 min in a microcentrifuge before beginning NMR data collection. Hydrogen exchange was monitored by collecting  $^{15}\text{N}$ -edited 1D spectra at 6 °C from 0.5 to 10.1 h after dissolving the protein (time points represent the midpoint of each data collection). Each of the 256 spectra contained 1024 data points and 128 scans. Using Azara (Wayne Boucher, Cambridge, England), the raw data were Fourier transformed after multiplication with a shifted sine function and zero filling. Peak intensities at 8.83, 8.48, 8.28, 8.19, 7.98, 7.83, and 7.73 ppm were determined using a modified version of Priism (28). Hydrogen exchange rates were determined by fitting the data to a single exponential ( $Ae^{-kt} + C$ ) using KaleidaGraph (Abelbeck). To ensure that no significant aggregation occurred during data collection, simple 1D,  $^1\text{H}$  spectra with 1024 data points, 32 dummy scans, and 64 scans were acquired before and after exchange. Previous attempts with 50 mM KCl in the solution failed due to aggregation.

**Urea-Dependent Quenched Hydrogen Exchange.** Quenched hydrogen exchange reactions and NMR sample preparation were carried out at 4 °C in a fashion similar to the experiments used to determine the structured regions of the acid state of RNase H (29). Lyophilized  $^{15}\text{N}$ -labeled RNase H (70–100 mg) was dissolved in 50 mL of deuterated exchange buffer (10 mM phosphoric acid, 50 mM KCl, pD 0.9–1.0) with 0.0, 0.2, 1.0, or 2.0 M urea and 110, 220, 370, or 700 mM DCl, respectively. After exchange out times ranging from 1 min to 26 h, 5 mL samples (7–10 mg RNase H), were diluted with a 7.5 mL deuterated “quench solution” of sodium acetate (0.20 M pD 5.5, 0.20 M pD 5.5, 0.35 M pD 5.5, or 0.5 M pD 6.8) in  $\text{D}_2\text{O}$ . The resulting solutions all had pD > 4, which allowed the protein to fold rapidly

into the native conformation. Samples were concentrated by Centrprep 10 (Amicon) to ~1 mL, diluted with 9 mL of 0.1 M deuterated sodium acetate pD 5.5 in D<sub>2</sub>O, and then concentrated to 0.5 mL. The pD was adjusted to 5.5 with NaOD for NMR data collection. The <sup>15</sup>N–<sup>1</sup>H HSQC spectra were collected within 24 h after quenching and processed as described (27). Hydrogen exchange rates were calculated by fitting the peak height as a function of time to a single exponential ( $Ae^{kt}$ ) using KaleidaGraph (Abelbeck). In addition to the HSQC spectra, 1D <sup>1</sup>H spectra were collected on each sample so that nonexchanging methyl protons could be used to normalize for variations in protein concentration.

Two control experiments were carried out on a 2.0 M urea sample to determine which protons could serve as probes of the molten globule structure. In the first, RNase H was dissolved in a protonated exchange solution (pH 1) and the quench was then carried out with deuterated quench solution (pH 6.8). In the second sample, protonated solutions were used at every step to ensure 100% protonation at every amide site. Amide protons whose exchange was not efficiently quenched will show a lower peak height in the first control sample than the corresponding peak in the second control sample. Probably due to poor H<sub>2</sub>O suppression in the second control sample's 1D spectrum which affected the normalization for protein concentration, the largest peaks in the first control spectrum contained only about 65% of the height of the second control spectrum. Our criteria for choosing probes of the molten globule state were to use protons (1) with more than 85% of the 65% peak height and (2) which exchanged less than 15% in 24 h in the native state (27).

**Analysis of Hydrogen Exchange Rates.** Hydrogen exchange rates were evaluated by the classic exchange reaction scheme shown in eq 1 (30–32). A “closed” amide site is



forbidden to exchange and must first undergo an opening transition before exchange occurs. The opening and closing rate constants are  $k_{\text{op}}$  and  $k_{\text{cl}}$ . The actual chemical exchange step is assumed to occur with the rate constant,  $k_{\text{ch}}$ , calculated from data on unstructured dipeptides (33). Exchange was assumed to follow EX2 kinetics where  $k_{\text{cl}} \gg k_{\text{ch}}$ , and the opening reaction is a preequilibrium step before the actual chemical exchange step. The observed exchange rate constant,  $k_{\text{obs}}$ , is given by

$$k_{\text{obs}} = k_{\text{ch}}K_{\text{op}}/(K_{\text{op}} + 1) = k_{\text{ch}}F_{\text{op}} \quad (2)$$

$K_{\text{op}}$  is the equilibrium constant for the opening reaction and  $F_{\text{op}}$  is the fraction of open protein molecules. This expression for  $k_{\text{obs}}$  describes the behavior of marginally stable species because there is no assumption that the closed state is much more populated than the open state.

For most protons, this formalism allows calculation of the free energy of hydrogen exchange,  $\Delta G_{\text{HX}} = -RT \ln K_{\text{op}}$  ( $R$  is the gas constant and  $T$  is the absolute temperature). However,  $\Delta G_{\text{HX}}$  is undefined if  $K_{\text{op}} < 0$ , as is the case for those protons in which the observed rate constant is actually faster than the rate predicted by the dipeptide data (33). Such fast rates may result from the dipeptide rates not actually reflecting the exchange rate in the completely open amide

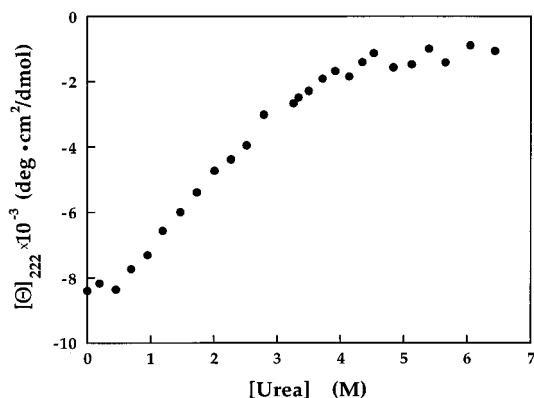


FIGURE 2: Urea denaturation of the RNase H molten globule. Denaturation was monitored by circular dichroism (CD) mean residue ellipticity at 222 nm in a deuterated solution, pD 0.8 and 4 °C.

site of RNase H or from noise inherent in the actual measurements. Therefore, we analyzed our data in terms of protection factors,  $P = k_{\text{ch}}/k_{\text{obs}}$  for all of the protons and determined  $\Delta G_{\text{HX}}$  where possible.  $\Delta G_{\text{HX}}$  refers to the  $\Delta G$  calculated from the hydrogen exchange rates, and  $\Delta G_{\text{UNF}}$ , “unfolding”, refers to the  $\Delta G$  determined by fitting  $\Delta G_{\text{HX}}$  as a function of urea to a line.

The pH and salt dependence of the molten globule forbid the standard verification of EX2 kinetics by altering the pH of exchange. EX2 kinetics hold when  $k_{\text{ch}} \ll k_{\text{cl}}$ . We assumed EX2 kinetics applied since the intrinsic chemical exchange rates are very slow at pH 1 and 4 °C (0.05–1.2 min<sup>−1</sup>) compared to the global refolding of the molten globule at pH 1 which occurs within the 50 ms mixing time of our stopped-flow CD/fluorimeter. If  $k_{\text{ch}} = k_{\text{cl}}$ , this would result in a 2-fold lower value of  $K_{\text{op}}$  and a corresponding increase in  $\Delta G_{\text{HX}}$  of only 0.38 kcal/mol for a given  $k_{\text{obs}}$ . The assumption is worse if  $k_{\text{cl}} < k_{\text{ch}}$ , but comparable values of  $k_{\text{ch}}$  and  $k_{\text{cl}}$  do not result in dramatically erroneous free energies.

## RESULTS

**Molten Globule State of RNase H.** The RNase H molten globule shares the flexibility and nonspecific packing found in other molten globules. Previously, we have shown that the urea-induced unfolding of the acid state of RNase H is very diffuse at 25 °C in H<sub>2</sub>O (6). Figure 2 shows that under the conditions of our hydrogen exchange measurements (4 °C, D<sub>2</sub>O) the molten globule state also shows a broad denaturation curve with little apparent sigmoidal shape, consistent with a noncooperative ensemble of structures. At the highest urea concentration used in our exchange experiments (2.0 M), the molten globule has lost about half its original CD signal at 222 nm, and therefore this amount of urea greatly affects the average amount of structure.

The chemical shift dispersion in the molten globule state of RNase H was assessed in a <sup>15</sup>N – <sup>1</sup>H heteronuclear single quantum coherence (HSQC) spectrum. As shown in Figure 3, the molten globule state of RNase H does not show the dispersion in the proton dimension characteristic of amide hydrogens having specific tertiary contacts and unique chemical environments. Although RNase H contains 155 amino acids, there are only about 70 discernible peaks in the HSQC spectrum. Many peaks are absent due to the

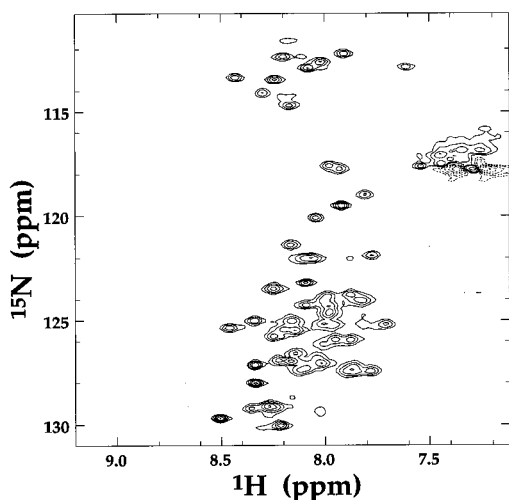


FIGURE 3: HSQC spectrum of the molten globule state of RNase H. The spectrum was taken at pH 1, 6 °C and displays the lack of dispersion in the  $^1\text{H}$  dimension characteristic of molten globules. Approximately 70 of the 153 expected amide backbone peaks are discernible. Peaks lying outside the spectrum, most likely Arg side chains, were aliased and appear as negative peaks (dashed lines).

severe overlap, transient intermolecular association, or intermediate exchange of the amide's chemical environment.

**Direct Hydrogen Exchange Measurements.** Amide hydrogen exchange was measured directly on the molten globule state with a series of  $^{15}\text{N}$ -edited  $^1\text{H}$  spectra. Since we could not obtain single-residue dispersion, exchange rates were calculated as the change in signal intensity of a particular peak, and may represent averages of the exchange behavior. Although we do not have assignments for the observed nuclei, these results allowed us to determine if any of the observable protons are well-protected. The observed subset of protons in this direct experiment is different than the subset monitored in the quenched experiment (below).

The first spectrum of the series (Figure 4a) shows that within the time needed to dissolve the sample and collect the first spectrum ( $\sim 30$  min), much of the signal is lost and the signal-to-noise ratio is quite low. By the last spectrum, collected after 10.1 h of exchange, no proton signals were discernible from the noise. Figure 4b shows the exchange kinetics of two peaks, at 8.19 and 7.73 ppm. All seven peaks analyzed exchanged with similar rates ( $0.017$ – $0.020 \text{ min}^{-1}$ ). The average observed exchange rate,  $k_{\text{obs}}$ , was  $0.018 \text{ min}^{-1}$ . These rates correspond to protection factors,  $P = k_{\text{ch}}/k_{\text{obs}}$ , ranging from 3 to 100 depending on the amide site used in the calculation. This range of low protection factors is consistent with, but slightly lower than the range determined in the quenched exchange experiments described previously (29) and below.

**Quenched Hydrogen Exchange with Denaturant.** To analyze the stability of individual regions of the protein in the molten globule state, we carried out quenched hydrogen exchange measurements as a function of urea. Quenching exchange by returning to the native state allowed us to use the native state assignments to identify the peaks. With this technique, we are limited to observing only those protons that exchange slowly in the native state. The observed rates were converted into the free energy of hydrogen exchange,  $\Delta G_{\text{HX}}$ , as described in Materials and Methods.

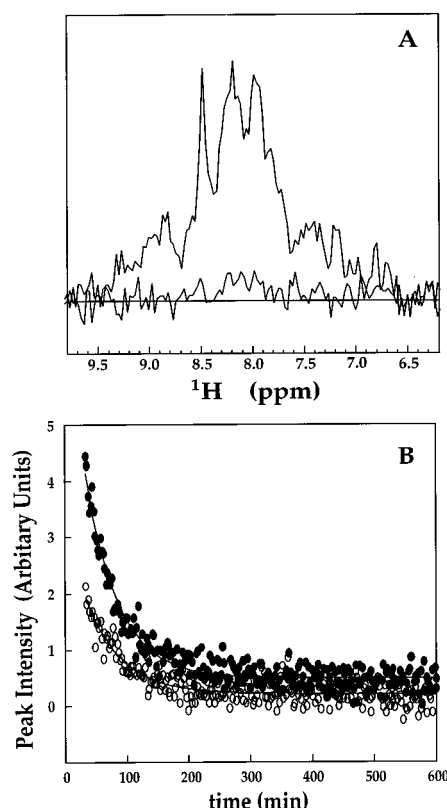


FIGURE 4: Hydrogen exchange measured directly on the molten globule state. Exchange was carried out at pD 0.9, 6 °C. (a) The first (30 min) and last (600 min)  $^{15}\text{N}$ -edited  $^1\text{H}$  spectra are shown. (b) The intensities of two representative peaks, 8.19 and 7.73 ppm, are shown as a function of time. The rate constants at all seven ppm values monitored were similar with the average  $k_{\text{obs}} = 0.018 \text{ min}^{-1}$ .

The five representative protons shown in Figure 5a exemplify the stability of different regions of the molten globule. Helix A (L56, closed circles) showed the greatest stability, with less stability shown in helix D (A109, squares), and strand 4 (L67, triangles). Helix E and strand 2 show comparable protection to strand 4. The remainder of the molecule shows no significant protection such as in strand 3 (F35, diamonds) and strand 5 (E119, open circles). In the absence of denaturant, the stability values ranged from below detection to 4.1 kcal/mol, corresponding to protection factors between 0.4 and 880. These protection factors are slightly higher than those reported previously (6). The lowest protection factor of 0.4 (E119) is not surprising given the recent report of  $k_{\text{ch}}$  values being underestimated for glutamate residues in an unfolded fragment of staphylococcal nuclease (34).

The free energy of hydrogen exchange showed a linear dependence on denaturant for every measurable proton in RNase H (Figure 5a). The  $m$  values of some protons are poorly determined since they were influenced by the larger noise inherent in calculating low  $\Delta G_{\text{HX}}$  values.  $\Delta G_{\text{UNF}}(\text{H}_2\text{O})$ , the stability determined by fitting  $\Delta G_{\text{HX}}$  vs denaturant, and  $m$  values are shown in Figure 5b for the well-determined protons and are listed with the protection factors in Table 1 for all protons monitored. The well determined  $m$  values range from 0.7 to 1.4 kcal/mol/M and appear to correlate with the stability of each residue,  $\Delta G_{\text{HX}}$ , particularly in helix A.

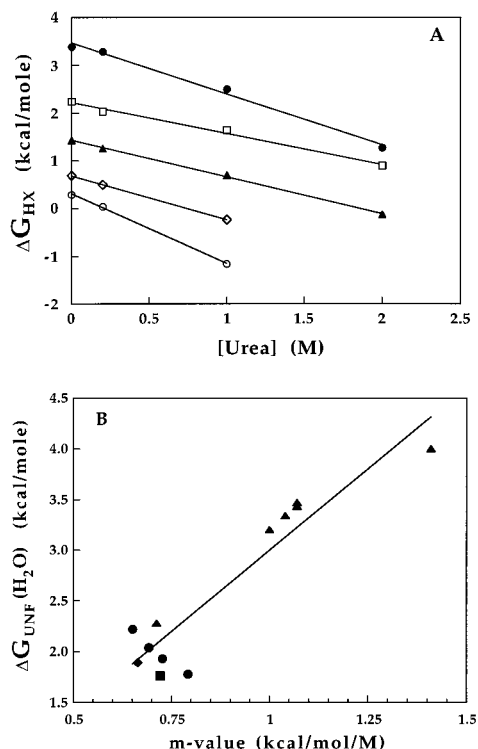


FIGURE 5: Quenched hydrogen exchange with increasing urea. (a) The free energy of hydrogen exchange,  $\Delta G_{HX}$ , is plotted for five representative protons as a function of urea concentration. The exchange of amide protons of L56 (helix A, closed circles), A109 (helix D, squares), L67 (strand 4, triangles), F35 (strand 3, diamonds), and E119 (strand 5, open circles) are shown.  $\Delta G_{HX}$  measurements are inaccurate below  $\Delta G_{HX} = 0$  kcal/mol because slight changes in rate constants create large variations in  $\Delta G_{HX}$ . (b) The free energy of unfolding in the absence of denaturant,  $\Delta G_{UNF}(H_2O)$ , is plotted as a function of  $m$  value for protons with well-determined  $m$  values. The  $m$  values were considered to be well determined if the protection factors were greater than 2 ( $\Delta G_{HX} > 0$ ) at all urea concentrations monitored. The symbols represent different areas of the protein: helix A (triangles), helix D (circles), helix B (square), and strand 2 (diamond). The best linear fit to the data shown is drawn.

## DISCUSSION

**Hydrogen Exchange as a Function of Denaturant.** The advantage of monitoring hydrogen exchange as a function of denaturant, or other perturbant, is to separate the two types of hydrogen exchange behavior that we refer to as “fluctuations” and “unfolding” reactions. Unfolding reactions are promoted by denaturant in contrast to fluctuations, which we define as insensitive to denaturants. Unfolding events represent large protein motions that expose new surface area, whereas local fluctuations may suggest that the native conformation breathes and cannot fully protect the amide proton in question. The native proteins studied to date, ribonuclease A (14), bovine pancreatic trypsin inhibitor (15), cytochrome C (16), chymotrypsin inhibitor 2 (20, 21), and RNase H (27), exhibit exchange through both unfolding events and fluctuations. The hydrogen exchange rates of barnase were also monitored as a function of denaturant (18), but the results were complicated by influences from EX1 kinetics.

In contrast to the results obtained on native proteins, the hydrogen exchange characteristics of each amide proton in the molten globule state of RNase H can be completely

Table 1: Hydrogen Exchange Characteristics of the Molten Globule State<sup>a</sup>

amino acid	location	$\Delta G_{UNF}(H_2O)$ , kcal/mol	$m$ value, kcal/mol/M	$P$			
				0.0 M	0.2 M	1.0 M	2.0 M
I7	strand 1	0.5	(0.9)	3.4	3.0	1.5	0.8
F8	strand 1	0.4	(1.4)	3.1	2.2	1.2	0.6
G20	strand 2	0.9	(0.8)	6.2	4.3	2.1	0.8
G21	strand 2	1.6	(0.9)	18	15	6.8	1.7
Y22	strand 2	1.5	(0.8)	14	11	5.3	1.6
A24	strand 2	1.9	0.7	34	22	12	3.6
I25	strand 2	0.8	(0.5)	5.7	5.0	2.2	1.7
L26	strand 2	0.5	(1.0)	3.6	2.9	1.4	0.7
R27	strand 2	1.1	(0.8)	8.4	6.0	2.7	1.4
F35	strand 3	0.7	(0.9)	4.5	3.5	1.6	0.9
R46	helix A	2.3	0.7	68	44	22	5.5
A51	helix A	3.3	1.0	400	340	69	11
A52	helix A	3.2	1.0	300	270	58	9.5
V54	helix A	4.0	1.4		620	210	7.4
A55	helix A	3.4	1.1	440	370	90	10
L56	helix A	3.5	1.1	480	400	99	11
I66	strand 4	1.5	(0.8)	16	12	4.3	1.8
L67	strand 4	1.4	(0.8)	15	11	4.6	1.8
S68	strand 4	1.8	0.7	25	17	10	2.6
W104	helix D	2.0	0.7	46	27	15	4.1
Q105	helix D	1.5	(0.9)	16	10	4.4	1.5
L107	helix D	1.8	0.8	31	17	7.1	2.5
A109	helix D	2.2	0.7	61	42	21	6.1
A110	helix D	1.9	0.7	38	27	9.1	3.5
K117	strand 5	0.7	(0.9)	5.2	3.4	1.8	0.9
E119	strand 5	0.3	(1.5)	2.7	2.1	1.1	0.4
L136	helix E	1.1	(0.5)	8.5	6.3	3.7	2.0
A139	helix E	1.4	(0.8)	14	9.4	4.6	1.6
A140	helix E	1.7	(0.9)	21	15	6.7	1.8

<sup>a</sup>  $\Delta G_{UNF}(H_2O)$ , free energy of unfolding in the absence of denaturant.  $m$  value, slope of  $\Delta G_{UNF}$  vs. urea.  $P$ , protection factor. The  $m$  values in parentheses were poorly determined due to the low protection factors,  $P < 2$ , in either 1.0 or 2.0 M urea.

described with only one type of exchange behavior, an unfolding reaction. For every amide proton measured, the free energy of hydrogen exchange decreased linearly with increasing denaturant concentration. Apparently, the internal motions allowing exchange in the molten globule state are large enough to be sensitive to denaturant and, therefore, must expose new surface area (22). The free energies for these unfolding events in the absence of denaturant,  $\Delta G_{UNF}(H_2O)$ , are low, ranging from below detection up to 4.1 kcal/mol compared to 6.5–11.1 kcal/mol in the native state (27). Therefore, these unfolding reactions are less energetically costly and occur more frequently in the molten globule state than in the native state.

The low levels of protection observed in the molten globule state made accurate determination of the  $m$  values difficult. For small values of  $\Delta G_{HX}$ , small changes in  $k_{obs}$  have a more pronounced effect on the calculated  $\Delta G_{HX}$ . For protons with protection factors less than 2 in either 1.0 or 2.0 M urea, the calculated  $m$  values were considered unreliable, because they were strongly biased by the uncertainty in the high urea measurements. The  $\Delta G_{UNF}(H_2O)$  and  $\Delta G_{HX}(H_2O)$  values, however, are more reliable since these protons were better protected at lower urea concentrations.

The variation seen in both stability ( $\Delta G_{UNF}(H_2O)$ ) and denaturant sensitivity ( $m$  values) implies that individual regions in the molten globule behave independently and the molten globule of RNase H is not folded cooperatively. The  $m$  values of protons within helix A, the most stable region

of the molten globule state, range from 0.7 to 1.4 kcal/mol/M. These values can be compared to an average  $m$  value of 0.023 kcal/mol/M for the unfolding of one helical residue in a peptide (35) and 0.58 to 3.7 kcal/mol/M for native proteins (22). For those protons whose  $m$  values we considered reliable, the  $m$  values appear to correlate linearly with the stability,  $\Delta G_{\text{UNF}}(\text{H}_2\text{O})$  (Figure 5b). For native proteins,  $m$  values correlate with the surface area exposed during unfolding, suggesting that more surface area is exposed when unfolding allows amide hydrogens with higher stabilities to exchange (22). Using models of unfolded proteins and their known crystal structures, Myers et al. (22) determined a relationship between the change in surface area upon unfolding and  $m$  values of native proteins:  $m = 0.11\Delta(\text{surface area}) + 374$ , where  $m$  is the  $m$  value in cal/mol/M and  $\Delta(\text{surface area})$  is the change in surface area upon unfolding in  $\text{\AA}^2$ . Assuming this equation also describes molten globules, we calculate that the hydrogen exchange opening reactions expose an additional 2500–10 000  $\text{\AA}^2$  of surface area in the RNase H molten globule. This area range is comparable to, but smaller than, the area exposed during the global unfolding of the native state (13,700  $\text{\AA}^2$ ) (22). These sizable  $m$  values imply that the motions detected by hydrogen exchange in the molten globule are large even though the molten globule is unstable and unfolds noncooperatively.

**The EX2 Assumption.** To calculate the stability of each amide hydrogen, we assumed EX2 kinetics in which  $k_{\text{ch}} < k_{\text{cl}}$ . Because of the sensitivity of the molten globule to changes in salt concentrations and the extremely low pH necessary, we could not verify EX2 kinetics by measuring the exchange rates as a function of pH. EX1 kinetics are unlikely since the intrinsic chemical exchange rates ( $k_{\text{ch}}$ ) are slow at pH 1 and 4 °C, ranging from 0.05 to 1.2  $\text{min}^{-1}$ . Any closing reaction for hydrogen exchange should be at least as fast as the global refolding of the molten globule at pH 1 which occurs in the mixing time of our stopped-flow apparatus ( $\sim 50$  ms) (data not shown). Additionally, the rate constants we observed in the quenched exchange experiment varied and did not converge to a common value as seen for protons in the native state of barnase that exchange through EX1 kinetics (18).

**Direct Hydrogen Exchange.** Despite the variation in protection factors measured in these and previous quenched hydrogen exchange experiments, our direct hydrogen exchange on the molten globule resulted in identical exchange rates for each peak. The most likely explanation for this narrow range of  $k_{\text{obs}}$  in the direct experiment is the severe overlap of proton resonances in the 1D spectra: the rate of decay of each peak in the 1D spectrum is averaged over many protons, and thus the rate constants have converged to a similar value. The presence of many nuclei with overlapping chemical shifts would result in multiphasic kinetics only if the time constants of each phase varied significantly.

**Comparison to Previous Studies on the Molten Globule State of RNase H.** Last year we carried out a similar quenched hydrogen exchange experiment to determine the structured regions of the molten globule state of RNase H in the absence of denaturant (29). The protection factors determined in the study presented here are slightly larger than those reported previously ( $P = 880$  vs  $P = 340$ ). The

experiments were done separately using different protein preparations, spectrometers, pulse sequences, and data processing. Although the exchange process and quench were similar, the protein samples were lyophilized from different salt conditions. The larger protection factors were found in the experiments containing the higher salt concentrations. Although salt effects on the RNase H molten globule are not currently known, the additional salt could reduce the charge repulsion responsible for creating the molten globule state and stabilize the interactions which protect the amide sites from exchange.

**Comparison with the Molten Globule State of  $\alpha$ -Lactalbumin.** It is informative to compare the native and molten globule states of RNase H to the well-studied, molten globule state of  $\alpha$ -lactalbumin. Protection factors for both molten globule states range into the hundreds (7), implying that the most stable regions of each molten globule have comparable stability. In RNase H, the most stable region in the molten globule is also the most stable region in the native state (27) based on hydrogen exchange experiments carried out as a function of denaturant (16). In contrast, Schulman et al. concluded that for  $\alpha$ -lactalbumin different regions of the protein were most stable in the molten globule (helix B) and native states (helix C) (7). Since their estimates of native state stability were based simply on protection factors in the absence of denaturant, it is possible that the relative stabilities of different regions in the  $\alpha$ -lactalbumin molten globule and native state are more similar. However, assuming there are no striking differences in the hydrogen exchange behavior of  $\alpha$ -lactalbumin native state measured with and without denaturant, the relative stabilities of different regions in the molten globule and native states appear to be a fundamental difference between  $\alpha$ -lactalbumin and RNase H.

Recently, Schulman et al. (36) followed the unfolding of the molten globule state of  $\alpha$ -lactalbumin using NMR spectroscopy. They concluded that individual regions in the molten globule of  $\alpha$ -lactalbumin behaved independently and the protein unfolded noncooperatively, as shown here for RNase H. They studied denaturation of the  $\alpha$ -lactalbumin molten globule by monitoring HSQC peaks as they became observable upon the addition of denaturant. Without denaturant, an HSQC spectrum of  $\alpha$ -lactalbumin's molten globule shows only three peaks corresponding to the first three backbone amides. More amide peaks were assigned as they became visible at their unfolded chemical shifts by the addition of denaturant.

An HSQC spectrum of the RNase H molten globule without denaturant (Figure 3) shows many more peaks ( $\sim 70$ ) than  $\alpha$ -lactalbumin. The assignments of these peaks are unknown. The molten globule state of RNase H may have very structured regions which could give rise to the discernible peaks. Alternatively, the visible peaks may correspond to unfolded regions of the protein as seen in  $\alpha$ -lactalbumin. This interpretation is supported by the similarity in protection factors to  $\alpha$ -lactalbumin, the lower protection observed in the directly monitored exchange experiment, and the lack of chemical dispersion of the molten globule HSQC. This would imply that the molten globule of RNase H has a greater number of completely unfolded amides sites than  $\alpha$ -lactalbumin. Hence, the most stable regions in the RNase H and  $\alpha$ -lactalbumin molten globules have comparable stability, but RNase H may have a much larger amount of

disordered amide sites possibly due to its lack of disulfide bonds.

**Summary.** We analyzed the characteristics of individual regions within the RNase H molten globule state by monitoring its hydrogen exchange behavior as a function of denaturant concentration. Every amide site measured in the molten globule undergoes low energy, opening events large enough to be sensitive to denaturant unlike native states of proteins which undergo separable unfolding events and local fluctuations. The molten globule of RNase H may also undergo smaller amplitude motions but these motions are not reflected in the hydrogen exchange data. Individual amide sites show very different stabilities and denaturant sensitivities, implying that each region of the molten globule behaves independently demonstrating the noncooperative unfolding of the molten globule state.

## ACKNOWLEDGMENT

The authors wish to thank Tracy M. Handel for use of the NMR spectrometer, David A. Agard for modifications to Priism for NMR peak fitting, Tanya M. Raschke for assistance with stopped-flow measurements, and the Marqusee laboratory for helpful discussions.

## REFERENCES

1. Kuwajima, K. (1989) *Proteins* 6, 87–103.
2. Ptitsyn, O. B., et al. (1990) *FEBS Lett.* 262, 20–24.
3. Jennings, P. A., and Wright, P. E. (1993) *Science* 262, 892–896.
4. Raschke, T. M., and Marqusee, S. (1997) *Nat. Struct. Biol.* 4, 298–304.
5. Hughson, F. M., Wright, P. E., and Baldwin, R. L. (1990) *Science* 249, 1544–1548.
6. Dabora, J. M., and Marqusee, S. (1994) *Protein Sci.* 3, 1401–1408.
7. Schulman, B. A., et al. (1995) *J. Mol. Biol.* 253, 651–657.
8. Woodward, C. K. (1994) *Curr. Opin. Struct. Biol.* 4, 112–116.
9. Englander, S. W., et al. (1996) *Curr. Opin. Struct. Biol.* 6, 18–23.
10. Zahn, R., et al. (1996) *Science* 271, 642–645.
11. Gervasoni, P., et al. (1996) *Proc. Natl. Acad. Sci. U.S.A.* 93, 12189–12194.
12. Goldberg, M. S., et al. (1997) *Proc. Natl. Acad. Sci. U.S.A.* 94, 1080–1085.
13. Niebla-Axmann, S. E., et al. (1997) *J. Mol. Biol.* 271, 803–818.
14. Mayo, S. L., and Baldwin, R. L. (1993) *Science* 262, 873–876.
15. Kim, K. S., Fuchs, J. A., and Woodward, C. K. (1993) *Biochemistry* 32, 9600–9608.
16. Bai, Y., et al. (1995) *Science* 269, 192–197.
17. Bai, Y., and Englander, S. W. (1996) *Proteins* 24, 145–151.
18. Clarke, J., and Fersht, A. R. (1996) *Folding Des.* 4, 243–254.
19. Chamberlain, A. K., and Marqusee, S. (1997) *Structure* 5, 859–863.
20. Itzhaki, L. S., Neira, J. L., and Fersht, A. R. (1997) *J. Mol. Biol.* 270, 89–98.
21. Neira, J. L., et al. (1997) *J. Mol. Biol.* 270, 99–110.
22. Myer, J. K., Pace, C. N., and Scholtz, J. M. (1995) *Protein Sci.* 4, 2138–2148.
23. Glasoe, P. F., and Long, F. A. (1960) *J. Phys. Chem.* 64, 188–193.
24. Norwood, T. J., et al. (1990) *J. Magn. Reson.* 488–501.
25. Bax, A., et al. (1990) *J. Magn. Reson.* 86, 304–318.
26. Grzesiek, S., and Bax, A. (1993) *J. Am. Chem. Soc.* 115, 12593–12594.
27. Chamberlain, A. K., Handel, T. M., and Marqusee, S. (1996) *Nat. Struct. Biol.* 3, 782–787.
28. Chen, H., et al. (1996) *J. Struct. Biol.* 116, 56–60.
29. Dabora, J. M., Pelton, J. G., and Marqusee, S. (1996) *Biochemistry* 35, 11951–11958.
30. Hvidt, A., and Nielsen, S. O. (1966) *Adv. Protein Chem.* 21, 288–386.
31. Woodward, C., Simon, I., and Tuchsén, E. (1982) *Mol. Cell. Biochem.* 48, 135–160.
32. Englander, S. W., and Kallenbach, N. R. (1983) *Q. Rev. Biophys.* 16, 521–655.
33. Bai, Y., et al. (1993) *Proteins* 17, 75–86.
34. Mori, S., van Zijl, P. C., and Shortle, D. (1997) *Proteins* 28, 325–332.
35. Scholtz, J. M., et al. (1995) *Proc. Natl. Acad. Sci. U.S.A.* 92, 185–189.
36. Schulman, B. A., et al. (1997) *Nat. Struct. Biol.* 4, 630–634.
37. Katayanagi, K., et al. (1990) *Nature* 347, 306–309.

BI972692I